Spectral singularities of odd-$\mathcal{PT}$-symmetric potentials

Vladimir V. Konotop[1] and Dmitry A. Zezyulin[2]
[1]*Departamento de Física and Centro de Física Teórica e Computacional, Faculdade de Ciências, Universidade de Lisboa, Campo Grande 2, Edifício C8, Lisboa 1749-016, Portugal*
[2]*ITMO University, St. Petersburg 197101, Russia*

(Received 13 November 2018; published 14 January 2019)

We describe one-dimensional stationary scattering of a two-component wave field by a non-Hermitian matrix potential which features odd-$\mathcal{PT}$ symmetry, i.e., symmetry with $(\mathcal{PT})^2 = -1$. The scattering is characterized by a 4×4 transfer matrix. The main attention is focused on spectral singularities which are classified into two types. Weak spectral singularities are characterized by the zero determinant of a diagonal 2×2 block of the transfer matrix. This situation corresponds to the lasing or coherent perfect absorption of pairs of oppositely polarized modes. Strong spectral singularities are characterized by a zero diagonal block of the transfer matrix. We show that in odd-$\mathcal{PT}$-symmetric systems any spectral singularity is self-dual, i.e., lasing and coherent perfect absorption occur simultaneously. A detailed analysis is performed for a case example of a $\mathcal{PT}$-symmetric coupler consisting of two waveguides, one with localized gain and another with localized absorption, which are coupled by a localized antisymmetric medium. For this coupler, we discuss weak self-dual spectral singularities and their splitting into complex-conjugate eigenvalues which represent bound states characterized by propagation constants with real parts lying in the continuum. A rather counterintuitive restoration of the unbroken odd-$\mathcal{PT}$-symmetric phase subject to the increase of the gain-and-loss strength is also revealed. A comparison between odd- and even-$\mathcal{PT}$-symmetric couplers, the latter characterized by $(\mathcal{PT})^2 = 1$, is also presented.

DOI: 10.1103/PhysRevA.99.013823

I. INTRODUCTION

Spectral characteristics of waves interacting with a medium having gain or losses can feature singularities. When this happens, it is possible to observe complete absorption of incident waves or emission of radiation propagating away from the potential (in the absence of incident waves). Such a type of absorption was predicted in [1] (see also [2]) for electromagnetic waves incident on an absorbing layer. Later total absorption and lasing were obtained for layered media [3]. The current growing interest in the subject has been triggered by recent works [4], where the term coherent perfect absorption (CPA) was introduced. Nowadays the phenomenon is studied in many physical settings [5].

Spectral singularities (SSs) represent wave numbers at which the reflection and transmission coefficients become infinite [6,7]. More generally, SSs in continuous spectra of non-Hermitian operators can be defined as real poles of the resolvent, and in the mathematical literature they have been known and studied for several decades [8]. If a SS is a real positive pole of the resolvent, it allows for a coherent lasing solution [9,10]. A SS at a negative wave number corresponds to CPA [4]. A CPA solution can also be viewed as an antilaser, i.e., a time-reversed lasing solution [4,5], and therefore the respective SS is often referred to as a time-reversed SS. When a system obeys parity-time ($\mathcal{PT}$) symmetry [11], a SS and time-reversed SS appear at the same wavelength [9,12]. This means that in a $\mathcal{PT}$-symmetric system any spectral singularity is self-dual and the system can operate as a laser and as a coherent perfect absorber simultaneously at the given wavelength. Apart from $\mathcal{PT}$-symmetric potentials, there exist other situations where self-dual spectral singularities also occur [10,13].

A non-Hermitian Hamiltonian with a SS is nondiagonalizable [14]. This resembles a similar property of Hamiltonians featuring exceptional points [15] which correspond to the situation where two eigenvalues from the discrete spectrum and the corresponding eigenvectors coalesce subject to the change of some control parameter of the system. The analogy between SSs and exceptional points can be extended further, since both of these phenomena may correspond to the transition from purely real to complex spectra of the Hamiltonian (also known as the transition from the unbroken to the broken $\mathcal{PT}$-symmetric phase). Indeed, it is well known [16] that, subject to the change of some control parameter, a $\mathcal{PT}$-symmetric system can be driven to an exceptional point, where two isolated eigenvalues coalesce and form a double eigenvalue associated with a Jordan block (which means that there is only one linearly independent eigenfunction associated with the double eigenvalue). Past the exceptional point, the double eigenvalue splits into a pair of simple complex-conjugate eigenvalues. In a similar way, a non-Hermitian system can undergo the transition from a purely real to a complex spectrum if changing some of its parameters triggers a self-dual spectral singularity in the continuous spectrum [13]. Past the self-dual spectral singularity, a pair of complex-conjugate eigenvalues emerges from an interior point of the continuous spectrum. This represents an alternative scenario of the $\mathcal{PT}$ phase breaking [13,17].

An antilinear time-reversal operator $\mathcal{T}$ can be implemented in physically different ways [18]. The first one corresponds to the conventional bosonic time reversal characterized by the property $\mathcal{T}^2 = 1$. This is the most used $\mathcal{T}$ operator in numerous applications of $\mathcal{PT}$ symmetry in quantum mechanics [11] and in other fields [19]. The description of the state of the art given above refers precisely to this case, which will be also termed as even-$\mathcal{PT}$ symmetry in what follows. In the meantime, an alternative fermionic time reversal, characterized by the property $\mathcal{T}^2 = -1$, has also been introduced in the theory of non-Hermitian systems [20,21], but so far it has received much less attention. Recently, we have shown [22] that odd-$\mathcal{PT}$ symmetry (we use this term to distinguish the $\mathcal{PT}$ symmetry with $\mathcal{T}^2 = -1$ from the conventional even-$\mathcal{PT}$ symmetry with $\mathcal{T}^2 = 1$) naturally appears in modeling wave propagation in combined $\mathcal{PT}$-symmetric and anti-$\mathcal{PT}$-symmetric [23] media. The odd-$\mathcal{PT}$-symmetric model introduced in [22] was an example of a discrete optical system, allowing one to explore the effects related to the intrinsic degeneracy of the discrete spectrum, including $\mathcal{PT}$-symmetry breaking through exceptional points.

The goal of the present work is twofold. First, we introduce an odd-$\mathcal{PT}$-symmetric waveguiding system which takes into account diffraction (or dispersion) of waves. Second, we describe the scattering by a localized odd-$\mathcal{PT}$-symmetric potential, focusing on the emergence of spectral singularities.

The paper is organized as follows. The model is introduced in Sec. II. In Sec. III we address some general characteristics of scattering of two-component fields and discuss two types of SSs. Analysis of the properties of the transfer matrix and SSs in a system obeying odd-$\mathcal{PT}$ symmetry is presented in Sec. IV. In Sec. V we perform detailed analysis of the stationary scattering by a localized potentials in an odd-$\mathcal{PT}$-symmetric coupler and compare the results with those obtained for scattering by conventional (even-)$\mathcal{PT}$-symmetric potentials. The results are summarized and discussed in Sec. VI.

II. MODEL

We consider the one-dimensional stationary scattering problem for a two-component field $\boldsymbol{\psi} = (\psi_1, \psi_2)^{\mathsf{T}}$ (here and in the following the index T means transpose),

$$H\boldsymbol{\psi} = k^2\boldsymbol{\psi}, \tag{1}$$

where k is the spectral parameter and the Hamiltonian is given by

$$H = -\frac{d^2}{dx^2}\sigma_0 + \hat{U}, \quad \hat{U} = \begin{pmatrix} U_0(x) & V_2(x) \\ V_2(x) & U_1(x) \end{pmatrix}. \tag{2}$$

Here σ_0 is the 2×2 identity matrix and all entries of the complex-valued matrix potential $\hat{U}$ vanish at infinity:

$$\lim_{x\to\pm\infty} U_{0,1}(x) = 0, \qquad \lim_{x\to\pm\infty} V_2(x) = 0. \tag{3}$$

In order to impose specific conditions on the matrix potential $\hat{U}(x)$, we first recall the definitions of the space inversion $\mathcal{P}$ and odd-time-reversal $\mathcal{T}$ operators [18]

$$\mathcal{P}: x \to -x, \qquad \mathcal{T} = i\sigma_2\mathcal{K}, \tag{4}$$

where $\sigma_{1,2,3}$ are the Pauli matrices and $\mathcal{K}$ is the conventional elementwise complex conjugation $\mathcal{K}\boldsymbol{\psi} = \boldsymbol{\psi}^*$ (here and in the following an asterisk is used for complex conjugation

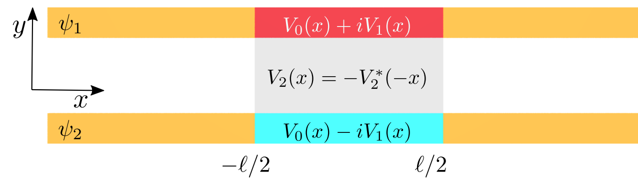

FIG. 1. Schematic of two waveguides which are locally coupled through an antisymmetric medium characterized by $V_2(x) = -V_2^*(-x)$. In the domain of coupling, the waveguides are doped by active impurities resulting in gain $+iV_1(x)$ and loss $-iV_1(x)$. A paraxial beam propagates along z axis directed toward the reader.

too). Obviously, $\mathcal{P}^2 = 1$, $\mathcal{T}^2 = -1$, $[\mathcal{P}, \mathcal{T}] = 0$, and hence $(\mathcal{PT})^2 = -1$ [in contrast to more-often-used even-parity-time reversals for which $(\mathcal{PT})^2 = 1$]. Note that the time-reversal operator is defined up to the phase factor, i.e., one can consider $\mathcal{T} = e^{i\varphi}\sigma_2\mathcal{K}$ with arbitrary real phase φ.

We require the Hamiltonian to be odd-$\mathcal{PT}$ symmetric, i.e., to satisfy

$$[H, \mathcal{PT}] = 0, \tag{5}$$

which is equivalent to the conditions

$$U_0(x) = U_1^*(-x), \qquad V_2(x) = -V_2^*(-x). \tag{6}$$

The latter condition requires the coupling $V_2(x)$ to be anti-$\mathcal{PT}$-symmetric, with the even-time-reversal operator being simply the complex conjugation $\mathcal{K}$ [23], which corroborates the coupled-waveguide model introduced in [22]. At the same time, as shown below in Sec. V, even a simpler case of real-valued $V_2(x)$ has physical meaning and leads to nontrivial results.

The model (1) and (2) with the Hamiltonian satisfying the requirements (5) and (6) may describe several physical settings. Recalling that optical couplers allow for simulating symmetries of almost any type (see, e.g., [24]), and hence of the odd-$\mathcal{PT}$ symmetry [22] too, below we interpret (13) as an odd-$\mathcal{PT}$-symmetric dispersive coupler. To this end, we consider two transparent planar waveguides located in the plane (x, z) and separated along the y axis as illustrated in Fig. 1. The dielectric permittivity of such a guiding medium is given by

$$\varepsilon_0\{1 + c_x(x)c_y(y) + \tilde{\varepsilon}(y + y_0)[f(x) + i\gamma(x)] + \tilde{\varepsilon}(y - y_0)[f(x) - i\gamma(x)]\}, \tag{7}$$

where $\tilde{\varepsilon}(y)$ is localized around $y = 0$ such that the overlap of $\tilde{\varepsilon}(y + y_0)$ and $\tilde{\varepsilon}(y - y_0)$ is negligible ($2y_0$ is the distance between the waveguide centers), the functions $\pm i\gamma(x)$ describe the distribution of gain and loss in the waveguides, $f(x)$ describes x-dependent distribution of the permittivity, $f(x)$ and $\gamma(x)$ are considered localized in the domain $|x| < \ell/2$, and the coupling between the waveguides, also localized in the interval $|x| < \ell/2$, is described by the complex function $c_x(x)c_y(y)$. Assuming the modulation of the dielectric permittivity to be sufficiently small, a monochromatic incident TE beam (i.e., the beam at $z = 0$) can be considered to be TE polarized at $z > 0$. Then the leading terms of the electric field are sought in the form

$$E = e^{i(\kappa^2/k_0)z - i\omega t}[\Psi_1(x, z)A_1(y) + \Psi_2(x, z)A_2(y)], \tag{8}$$

where $k_0 = \omega/c$, ω is the frequency, and $A_{1,2}(y)$ are the transverse modes of the respective waveguides. In our case $A_j(y) = A(y - (-1)^j y_0)$, where $A(y)$ is the eigenmode solving the spectral problem

$$\frac{d^2A}{dy^2} + \tilde{\varepsilon}_0(y)A = \kappa^2 A, \tag{9}$$

with κ^2 being a real spectral parameter. The modes are chosen to be normalized: $(A, A) = 1$ [we use the standard inner product $(A, B) = \int A^*(y)B(y)dy$]. The functions $\Psi_{1,2}$ are the field envelopes, which are slowly varying in the waveguide planes (i.e., in the planes $y = \pm y_0$).

Substituting (8) into the Helmholtz equation, in the paraxial approximation one obtains

$$i\frac{\partial\Psi_1}{\partial z} + \frac{\partial^2\Psi_1}{\partial x^2} - [V_0(x) + iV_1(x)]\Psi_1 - V_2(x)\Psi_2 = 0,$$
$$i\frac{\partial\Psi_2}{\partial z} + \frac{\partial^2\Psi_2}{\partial x^2} - [V_0(x) - iV_1(x)]\Psi_2 - V_2(x)\Psi_1 = 0. \tag{10}$$

Here we use dimensionless variables redefining $\sqrt{2}k_0x \to x$ and $k_0z \to z$, as well as the following definitions for the coefficients:

$$V_0(x) = -\frac{f(x)}{2}(A, \tilde{\varepsilon}A), \quad V_1(x) = -\frac{\gamma(x)}{2}(A, \tilde{\varepsilon}A). \tag{11}$$

The coupling is assumed to fulfill the requirement

$$V_2(x) = -\frac{c_x(x)}{2}(A_1, c_yA_2) = \frac{c_x^*(-x)}{2}(c_yA_2, A_1). \tag{12}$$

Finally, looking for stationary solutions $\Psi(z, x) = e^{i\beta z}\psi(x)$, we arrive at the scattering problem

$$-\psi_{1,xx} + [V_0(x) + iV_1(x)]\psi_1 + V_2(x)\psi_2 = k^2\psi_1,$$
$$-\psi_{2,xx} + [V_0(x) - iV_1(x)]\psi_2 + V_2(x)\psi_1 = k^2\psi_2, \tag{13}$$

where $k^2 = -\beta$. Thus we obtained the particular case of model (1) and (2), where $U_0(x) = U_1^*(x) = V_0(x) + iV_1(x)$.

The following observation is in order here. It follows from the explicit derivation of the model that eventual imaginary parts of the eigenvalues k^2, and thus the imaginary parts of the propagation constant β, correspond to solutions growing or decaying along the propagation distance z remaining localized in the waveguide planes (cf. [2]).

III. GENERAL FORMALISM

A. Jost solutions, transfer matrix, and scattering coefficients

First, we introduce some general definitions and scattering characteristics for the spinor system (1) and (2), which will be used below. No specific symmetry of the matrix potential $\hat{U}(x)$ is assumed so far, i.e., the condition (5) is not imposed in this section. It is yet assumed that all entries of $\hat{U}(x)$ are localized [i.e., Eqs. (3) hold] and tend to zero fast enough such that the continuous spectrum of scattering states occupies the real semiaxis $k^2 \geqslant 0$. As usual, the Jost solutions of the scattering problem (1) and (2) are defined by their asymptotics at $x \to -\infty$ (defined by $j = 1$) and at $x \to \infty$ (defined by $j = 2$):

$$\boldsymbol{\phi}_{1j}(x, k) \to \begin{pmatrix}1\\0\end{pmatrix}e^{ikx} = |\uparrow\rangle e^{ikx}, \tag{14a}$$

$$\boldsymbol{\phi}_{2j}(x, k) \to \begin{pmatrix}0\\1\end{pmatrix}e^{ikx} = |\downarrow\rangle e^{ikx}, \tag{14b}$$

$$\boldsymbol{\phi}_{3j}(x, k) \to \begin{pmatrix}1\\0\end{pmatrix}e^{-ikx} = |\uparrow\rangle e^{-ikx}, \tag{14c}$$

$$\boldsymbol{\phi}_{4j}(x, k) \to \begin{pmatrix}0\\1\end{pmatrix}e^{-ikx} = |\downarrow\rangle e^{-ikx}. \tag{14d}$$

The vectorial character of the two-component solutions makes it convenient to use the terminology of the up-polarized $|\uparrow\rangle$ and down-polarized $|\downarrow\rangle$ states. While we are primarily interested in the behavior of the system at real wave numbers k, the Jost solutions can be defined in the complex k plane by the analytic continuation from the real axis.

The 4×4 transfer matrix $M(k)$ and its inverse $M^{-1}(k)$ are introduced through the relations

$$\boldsymbol{\phi}_{j1}(x, k) = \sum_{m=1}^{4} M_{mj}(k)\boldsymbol{\phi}_{m2}(x, k), \tag{15}$$

$$\boldsymbol{\phi}_{j2}(x, k) = \sum_{m=1}^{4}(M^{-1})_{mj}(k)\boldsymbol{\phi}_{m1}(x, k). \tag{16}$$

Using standard arguments of the ordinary differential equation theory, one can prove that

$$\det M(k) = 1. \tag{17}$$

From the definition of the Jost functions, it is clear that both the transition and reflection of an incident polarized wave can occur with, $\alpha \to \beta$, and without, $\alpha \to \alpha$, inversion of polarization (here α and β stand for the states $\uparrow$ and $\downarrow$). Correspondingly, we introduce reflection $r_{\alpha\beta}$ and transmission $t_{\alpha\beta}$ coefficients, which are defined through the asymptotics of the solutions $\boldsymbol{\phi}_\alpha^{L,R}(x)$, where the upper indices L and R stand for left and right incidence, respectively. To define such solutions it is convenient to consider only positive $k > 0$ and identify the left $e^{ikx}|\alpha\rangle$ and right $e^{-ikx}|\alpha\rangle$ incident waves. Correspondingly, we have

$$\boldsymbol{\phi}_\uparrow^L \to \begin{cases} e^{ikx}|\uparrow\rangle + r_{\uparrow\uparrow}^L e^{-ikx}|\uparrow\rangle + r_{\uparrow\downarrow}^L e^{-ikx}|\downarrow\rangle, & x \to -\infty \\ t_{\uparrow\uparrow}^L e^{ikx}|\uparrow\rangle + t_{\uparrow\downarrow}^L e^{ikx}|\downarrow\rangle, & x \to +\infty, \end{cases}$$

$$\boldsymbol{\phi}_\downarrow^L \to \begin{cases} e^{ikx}|\downarrow\rangle + r_{\downarrow\downarrow}^L e^{-ikx}|\downarrow\rangle + r_{\downarrow\uparrow}^L e^{-ikx}|\uparrow\rangle, & x \to -\infty \\ t_{\downarrow\downarrow}^L e^{ikx}|\downarrow\rangle + t_{\downarrow\uparrow}^L e^{ikx}|\uparrow\rangle, & x \to +\infty, \end{cases}$$

$$\boldsymbol{\phi}_\uparrow^R \to \begin{cases} e^{-ikx}|\uparrow\rangle + r_{\uparrow\uparrow}^R e^{ikx}|\uparrow\rangle + r_{\uparrow\downarrow}^R e^{ikx}|\downarrow\rangle, & x \to +\infty \\ t_{\uparrow\uparrow}^R e^{-ikx}|\uparrow\rangle + t_{\uparrow\downarrow}^R e^{-ikx}|\downarrow\rangle, & x \to -\infty, \end{cases}$$

$$\boldsymbol{\phi}_\downarrow^R \to \begin{cases} e^{-ikx}|\downarrow\rangle + r_{\downarrow\downarrow}^R e^{ikx}|\downarrow\rangle + r_{\downarrow\uparrow}^R e^{ikx}|\uparrow\rangle, & x \to +\infty \\ t_{\downarrow\downarrow}^R e^{-ikx}|\downarrow\rangle + t_{\downarrow\uparrow}^R e^{-ikx}|\uparrow\rangle, & x \to -\infty. \end{cases}$$

Finally, comparing these asymptotics with the definitions (14)–(16), we can express the reflection and transmission coefficients through the elements of the transfer matrix. These expressions are presented in Appendix A.

B. Spectral singularities, CPA, and lasing

Now we turn to SSs and their physical implications. Since any scattering state $\boldsymbol{\psi}(x)$ from the continuous spectrum can be represented by a linear combination of the Jost solutions, in the limit $x \to -\infty$ it has the asymptotics

$$\boldsymbol{\psi}(x) \to a_1 e^{ikx}|\uparrow\rangle + a_2 e^{ikx}|\downarrow\rangle + a_3 e^{-ikx}|\uparrow\rangle + a_4 e^{-ikx}|\downarrow\rangle, \tag{18}$$

where a_j are coefficients, and for $k > 0$ the terms proportional to e^{ikx} and e^{-ikx} correspond to the waves propagating towards and away from the potential, respectively. Similarly, in the limit $x \to \infty$ the same scattering state behaves as

$$\boldsymbol{\psi}(x) \to b_1 e^{ikx}|\uparrow\rangle + b_2 e^{ikx}|\downarrow\rangle + b_3 e^{-ikx}|\uparrow\rangle + b_4 e^{-ikx}|\downarrow\rangle, \tag{19}$$

and for $k > 0$ the terms proportional to e^{ikx} and e^{-ikx} correspond to the waves propagating away from and towards the potential, respectively. Next, we observe that column vectors

$$\boldsymbol{a} = (a_1, a_2, a_3, a_4)^{\mathsf{T}}, \quad \boldsymbol{b} = (b_1, b_2, b_3, b_4)^{\mathsf{T}} \tag{20}$$

are related by the transfer matrix

$$\boldsymbol{b} = M\boldsymbol{a}. \tag{21}$$

Since the transfer matrix couples two right- and left-propagating waves with two polarizations, it is convenient to analyze its block representation

$$M(k) = \begin{pmatrix} \mathcal{M}_{11}(k) & \mathcal{M}_{12}(k) \\ \mathcal{M}_{21}(k) & \mathcal{M}_{22}(k) \end{pmatrix}, \tag{22}$$

where $\mathcal{M}_{ij}$ are 2×2 matrices. Indeed, the diagonal blocks $\mathcal{M}_{jj}$ describe total transmission, while the antidiagonal blocks $\mathcal{M}_{ij}$ $(i \neq j)$ describe total reflection.

Formally, SSs are determined by properties of the diagonal block $\mathcal{M}_{22}(k)$ at $k \in \mathbb{R}$. Since, however, $\mathcal{M}_{22}(-k) = \mathcal{M}_{11}(k)$ for any real k, below we consider SSs only at $k > 0$. This is convenient for the analysis of the reflection and transmission coefficients introduced above. Thus, in this approach, the time-reversed SS is determined by the properties of the block $\mathcal{M}_{11}(k)$ at $k > 0$.

It is evident from the formulas for the scattering data shown in Appendix A that their singularities are expected when

$$\Delta(k_\star) = 0, \tag{23}$$

where $\Delta(k) := \det \mathcal{M}_{22}(k)$ and $k_\star$ is real. The lasing corresponds to the existence of only outgoing solutions for a given $k = k_\star > 0$, i.e., to solutions $\psi_{\rm las}(x)$ whose asymptotic behavior in (18) and (19) is described by the column vectors

$$\boldsymbol{a}_{\rm las} = (0, 0, a_3, a_4)^{\mathsf{T}}, \quad \boldsymbol{b}_{\rm las} = (b_1, b_2, 0, 0)^{\mathsf{T}}. \tag{24}$$

For such solutions Eq. (21) reduces to

$$\mathcal{M}_{22}(k_\star)\begin{pmatrix} a_3 \\ a_4 \end{pmatrix} = 0_{2,1}, \tag{25a}$$

$$\begin{pmatrix} b_1 \\ b_2 \end{pmatrix} = \mathcal{M}_{12}(k_\star)\begin{pmatrix} a_3 \\ a_4 \end{pmatrix}, \tag{25b}$$

where $0_{m,n}$ stands for an $m\times n$ zero matrix.

Thus there exist two possibilities for realization of the lasing. The first one corresponds to the case when the determinant of matrix $\mathcal{M}_{22}(k_\star)$ is zero [i.e., $\Delta(k_\star) = 0$] but some of the matrix elements of $\mathcal{M}_{22}(k_\star)$ are nonzero. In this case the amplitudes of left-incident waves a_3 and a_4 are determined by Eq. (25a). Such a spectral singularity will be called weak. The second possibility corresponds to the case when all entries of the 2×2 block $\mathcal{M}_{22}$ are zero, i.e., $\mathcal{M}_{22}(k_\star) = 0_{2,2}$. This singularity will be referred to as strong; it corresponds to the arbitrary choice of the amplitudes $a_{3,4}$, including the cases when one of them is zero.

Similarly, the CPA corresponds to solutions

$$\boldsymbol{a}_{\rm CPA} = (a_1, a_2, 0, 0)^{\mathsf{T}}, \quad \boldsymbol{b}_{\rm CPA} = (0, 0, b_3, b_4)^{\mathsf{T}}, \tag{26}$$

i.e., to the conditions

$$\mathcal{M}_{11}(k_\star)\begin{pmatrix} a_1 \\ a_2 \end{pmatrix} = 0_{2,1}, \quad \begin{pmatrix} b_3 \\ b_4 \end{pmatrix} = \mathcal{M}_{21}(k_\star)\begin{pmatrix} a_1 \\ a_2 \end{pmatrix}. \tag{27}$$

Such $k_\star > 0$ is a time-reversed SS, which is either weak, when $\det \mathcal{M}_{11}(k_\star) = 0$ but $\mathcal{M}_{11}(k_\star) \neq 0_{2,2}$, or strong, when $\mathcal{M}_{11}(k_\star) = 0_{2,2}$.

In the case of a strong SS one has

$$\det M(k_\star) = -\det \mathcal{M}_{12}(k_\star)\, \det \mathcal{M}_{21}(k_\star). \tag{28}$$

This relation, together with Eq. (17), means that antidiagonal blocks $\mathcal{M}_{ij}(k_\star)$ are invertible. Using a similar argument, in the case of a weak SS, one can establish that antidiagonal blocks $\mathcal{M}_{ij}(k_\star)$ are nonzero matrices. However, their determinants in principle may acquire the zero value. For a given weak singularity let $\det \mathcal{M}_{12}(k_\star) = 0$. Then, at least one of the eigenvalues of $\mathcal{M}_{12}(k_\star)$ is zero. Also, let λ be the second eigenvalue (it can be zero too). Then, by the Schur decomposition, the nonzero matrix $\mathcal{M}_{12}(k_\star)$ by a unitary transformation Q can be reduced to the upper triangular matrix of the form

$$\mathcal{M}_{12}(k_\star) = Q\begin{pmatrix} 0 & \mu \\ 0 & \lambda \end{pmatrix}Q^{-1}, \tag{29}$$

where μ is a complex number. Hence, $[\mathcal{M}_{12}(k_\star)]^2 = \lambda\mathcal{M}_{12}(k_\star)$. Thus applying $\mathcal{M}_{12}(k_\star)$ to both sides of Eq. (25b), we obtain that $(b_1, b_2)^{\mathsf{T}}$ is an eigenvector of $\mathcal{M}_{12}(k_\star)$ corresponding to the eigenvalue λ. Similarly, if for some CPA solution one has $\det \mathcal{M}_{21}(k_\star) = 0$, then $(b_3, b_4)^{\mathsf{T}}$ is an eigenvector of $\mathcal{M}_{21}(k_\star)$.

Summarizing, for any CPA ($j = 1$) or lasing ($j = 2$) solution of the potential characterized by a transfer matrix with a noninvertible antidiagonal block $\mathcal{M}_{ij}$ $(i \neq j)$, the field from one side of the potential is an eigenvector of the diagonal block $\mathcal{M}_{jj}$, while the field from the opposite side of the potential is an eigenvector of the antidiagonal block.

IV. SELF-DUAL SPECTRAL SINGULARITIES

The definitions and properties described in the preceding section did not assume the system to admit any particular symmetry. In this section we use the odd-$\mathcal{PT}$ symmetry (5) to obtain additional information on the scattering properties.

Since the Jost solutions are defined uniquely by their asymptotics, odd-$\mathcal{PT}$ symmetry results in the relations

$$\mathcal{PT}\boldsymbol{\phi}_{11}(x,k) = i\boldsymbol{\phi}_{22}(x,k^*),$$
$$\mathcal{PT}\boldsymbol{\phi}_{31}(x,k) = i\boldsymbol{\phi}_{42}(x,k^*),$$
$$\mathcal{PT}\boldsymbol{\phi}_{21}(x,k) = -i\boldsymbol{\phi}_{12}(x,k^*),$$
$$\mathcal{PT}\boldsymbol{\phi}_{41}(x,k) = -i\boldsymbol{\phi}_{32}(x,k^*).$$

Using these formulas, one can establish the property

$$M^{-1}(k^*) = SM^*(k)S, \tag{30}$$

where $S = \sigma_0 \otimes \sigma_2$, which in the explicit form means that

$$M^{-1}(k^*) = \begin{pmatrix} M_{22}^* & -M_{21}^* & M_{24}^* & -M_{23}^* \\ -M_{12}^* & M_{11}^* & -M_{14}^* & M_{13}^* \\ M_{42}^* & -M_{41}^* & M_{44}^* & -M_{43}^* \\ -M_{32}^* & M_{31}^* & -M_{34}^* & M_{33}^* \end{pmatrix}, \tag{31}$$

where all matrix elements on the right-hand side are evaluated at k (not at k^*).

Now we prove that any SS, either weak or strong, is self-dual, i.e., that any SS at the wave number $k_\star$ is always accompanied by the time-reversed SS at the same wave number $k_\star$. As discussed above, for the strong SS with $\mathcal{M}_{22}(k_\star) = 0_{2,2}$, the matrices $\mathcal{M}_{12}$ and $\mathcal{M}_{21}$ are invertible. Thus, at $k = k_\star$ we have [25]

$$M^{-1} = \begin{pmatrix} 0_{2,2} & \mathcal{M}_{21}^{-1} \\ \mathcal{M}_{12}^{-1} & -\mathcal{M}_{12}^{-1}\mathcal{M}_{11}\mathcal{M}_{21}^{-1} \end{pmatrix}. \tag{32}$$

Comparing this expression with (30) [or (31)], we observe that the block 11 of M^{-1} has the form (below, the blocks of M^{-1} are denoted by $\tilde{\mathcal{M}}_{ij}$, with $i, j = 1, 2$)

$$\tilde{\mathcal{M}}_{11} = \begin{pmatrix} M_{22}^* & -M_{21}^* \\ -M_{12}^* & M_{11}^* \end{pmatrix}. \tag{33}$$

Thus $\mathcal{M}_{22}(k_\star) = 0_{2,2}$ implies $\mathcal{M}_{11}(k_\star) = 0_{2,2}$. The converse can be proven in a similar way: If $\mathcal{M}_{11}(k_\star) = 0_{2,2}$, then $\mathcal{M}_{22}(k_\star) = 0_{2,2}$.

Now we turn to weak singularities, i.e., assume that $\Delta(k_\star) = \det \mathcal{M}_{22}(k_\star) = 0$. Suppose that a weak SS is not self-dual, i.e., $\det \mathcal{M}_{11}(k_\star) \neq 0$. Since the entire transfer matrix $M(k_\star)$ is invertible, we conclude that there exists an invertible matrix $\mathcal{C}_1(k_\star)$, defined as

$$\mathcal{C}_1(k_\star) = \mathcal{M}_{22}(k_\star) - \mathcal{M}_{21}(k_\star)[\mathcal{M}_{11}(k_\star)]^{-1}\mathcal{M}_{12}(k_\star), \tag{34}$$

and the block 22 of the inverse matrix $M^{-1}(k_\star)$ is equal to $[\mathcal{C}_1(k_\star)]^{-1}$ [see [25] or formula (B2) in Appendix B]. On the other hand, as follows from (31), the determinant of this block is equal to $\det \mathcal{M}_{22}^*(k_\star)$ and the latter is equal to zero. Hence the determinant of $[\mathcal{C}_1(k_\star)]^{-1}$ is zero, which contradicts the invertibility of $\mathcal{C}_1(k_\star)$. The contradiction can be removed only if we admit that $\det \mathcal{M}_{11}(k_\star) = 0$. Therefore, $\det \mathcal{M}_{22}(k_\star) = 0$ implies $\det \mathcal{M}_{11}(k_\star) = 0$. The converse statement, i.e., that $\det \mathcal{M}_{11}(k_\star) = 0$ implies $\det \mathcal{M}_{22}(k_\star) = 0$, can be proven in a similar way, but employing the matrix

$$\mathcal{C}_2(k_\star) = \mathcal{M}_{11}(k_\star) - \mathcal{M}_{12}(k_\star)[\mathcal{M}_{22}(k_\star)]^{-1}\mathcal{M}_{21}(k_\star) \tag{35}$$

with the formula for the inverse of the block matrix (B3).

Thus, we have proven that both strong and weak spectral singularities are self-dual. This result extends the known property of spectral singularities of (even)-$\mathcal{PT}$-symmetric systems [9] to the case of odd-$\mathcal{PT}$ symmetry.

Alternatively, the self-dual nature of any spectral singularity can be established using the property of $\mathcal{PT}$ symmetry. Indeed, from the asymptotic behavior of lasing and CPA solutions it follows that applying the $\mathcal{PT}$ operator to a lasing solution with $k = k_\star$, one obtains a CPA one with the same wave vector $k_\star$ (and vice versa). Thus lasing and CPA always take place simultaneously, i.e., at the same wave vector $k_\star$.

Let us now assume the spectral parameter k to be complex valued and consider the matrix functions $\mathcal{M}_{ij}(k)$ defined in the complex plane. Let us also assume that the matrix potential $\hat{U}(x)$ depends on one or several real parameters, say, v_j ($j = 0, 1, \ldots$), and that $k_\star > 0$ is a (self-dual) weak spectral singularity for given values of the parameters, say, for $v_{\star j}$. Then, subject to the variation of some of the parameters v_j, the self-dual spectral singularity $k_\star$ either moves along the real axis remaining self-dual or disappears. The latter case corresponds to the situation when the zeros of $\det \mathcal{M}_{11}(k)$ and $\det \mathcal{M}_{22}(k)$ split [26] and move to the complex plane. As a result, a pair of complex-conjugate eigenvalues emerges in the spectrum of the Hamiltonian. Such a splitting of the self-dual spectral singularity into a complex-conjugate pair is one of the possible scenarios of the $\mathcal{PT}$-symmetry breaking, different from the coalescence of the discrete eigenvalues at an exceptional point [13].

Like in even-$\mathcal{PT}$-symmetric systems, the described splitting of a self-dual SS is constrained by the symmetry. Indeed, suppose that for some complex k_0 we have $\det \mathcal{M}_{22}(k_0) = 0$, but $\det \mathcal{M}_{11}(k_0^*) \neq 0$. Then, as follows from Appendix B, $\mathcal{C}_1(k_0^*)$ is invertible and the lower diagonal block of $M^{-1}(k_0^*)$ is equal to $[\mathcal{C}_1(k_0^*)]^{-1}$. However, from the explicit expression (31) it follows that the determinant of the latter block is equal to $[\det \mathcal{M}_{22}(k_0)]^*$, which is zero. This contradicts the invertibility of $\mathcal{C}_1(k_0^*)$. The contradiction can be lifted only if we admit that $\det \mathcal{M}_{11}(k_0^*) = 0$.

Similarly, one can prove that if $\det \mathcal{M}_{11}(k_0) = 0$, then $\det \mathcal{M}_{22}(k_0^*) = 0$. In other words, in a $\mathcal{PT}$-symmetric system, roots of $\det \mathcal{M}_{11}(k)$ and $\det \mathcal{M}_{22}(k)$ are either self-dual or complex conjugate.

V. EXAMPLE

A. Specific model

Now we turn to the specific model (13), considering

$$V_{0,1}(x) = V_{0,1}(-x), \quad V_2(x) = -V_2(-x), \tag{36}$$

where $V_0(x)$, $V_1(x)$, and $V_2(x)$ are real-valued functions (see also Fig. 1 for a schematic). According to (3), we require $\lim_{x\to\pm\infty} V_{0,1,2}(x) = 0$.

For the particular form of Hamiltonian (2) corresponding to the model (36) one can identify additional linear $\sigma_3\mathcal{P}$ and antilinear $\sigma_1\mathcal{K}$ symmetries

$$[H, \sigma_3\mathcal{P}] = [H, \sigma_1\mathcal{K}] = 0_{2,2}. \tag{37}$$

These symmetries lead to additional relations among the blocks of the transfer matrix $M(k)$, which means that only the upper blocks $\mathcal{M}_{11}$ and $\mathcal{M}_{12}$ are sufficient to know the entire transfer matrix (or its inverse). Indeed, $\sigma_1\mathcal{K}$ symmetry means that for real k the transfer matrix can be represented as

$$M = \begin{pmatrix} \mathcal{M}_{11} & \mathcal{M}_{12} \\ \sigma_1\mathcal{M}_{12}^*\sigma_1 & \sigma_1\mathcal{M}_{11}^*\sigma_1 \end{pmatrix}. \tag{38}$$

Using the symmetry $\sigma_3\mathcal{P}$ and the expression for the inverse transfer matrix (31), one obtains

$$M^{-1} = \begin{pmatrix} \sigma_2\mathcal{M}_{11}^*\sigma_2 & \sigma_2\mathcal{M}_{12}^*\sigma_2 \\ \sigma_3\mathcal{M}_{12}\sigma_3 & \sigma_3\mathcal{M}_{11}\sigma_3 \end{pmatrix}. \tag{39}$$

Furthermore, analyzing the 11 and 12 blocks of the identity $MM^{-1} = I$ (where I is 4×4 identity matrix), written in terms of (38) and (39), one obtains the matrix relations connecting blocks $\mathcal{M}_{11}$ and $\mathcal{M}_{12}$ expressed in terms of the matrices $\mathcal{N}_1 = \mathcal{M}_{11}\sigma_2$ and $\mathcal{N}_2 = \mathcal{M}_{12}\sigma_3$:

$$\mathcal{N}_1\mathcal{N}_2^* = \mathcal{N}_2\mathcal{N}_1, \tag{40a}$$

$$\mathcal{N}_2^2 - \mathcal{N}_1\mathcal{N}_1^* = \sigma_0. \tag{40b}$$

Let $\alpha_{1,2}(k)$ be the two eigenvalues of the matrix $\mathcal{N}_2(k)$. From Eq. (40b) we have that

$$|\det\mathcal{M}_{11}|^2 = \det\left(\sigma_0 - \mathcal{N}_2^2\right) = \left(1-\alpha_1^2\right)\left(1-\alpha_2^2\right). \tag{41}$$

Thus, any self-dual spectral singularity [i.e., the moment when $\det\mathcal{M}_{11}(k_\star) = \det\mathcal{M}_{22}(k_\star) = 0$] takes place when at least one of the eigenvalues of $\mathcal{M}_{12}\sigma_3$ is equal to either $+1$ or -1.

If k is not a spectral singularity, and thus $\mathcal{N}_1(k)$ is invertible, from Eq. (40a) we obtain that $\mathcal{N}_2$ and $\mathcal{N}_2^*$ are similar, i.e., they share the same eigenvalues which are either a complex-conjugate pair or both real. In the latter case they must satisfy $\alpha_{1,2} > 1$ or $\alpha_{1,2} < 1$. Thus, if k is not a spectral singularity, then $\det\mathcal{M}_{12}(k) = -\det\mathcal{N}_2(k)$ is real.

Let now $k = k_\star$. Consider a CPA solution. From the relation $\boldsymbol{a} = M^{-1}\boldsymbol{b}$ [see (21)] and from the explicit expressions (38) and (39) one can deduce that

$$\mathcal{N}^2\tilde{\boldsymbol{b}} = \tilde{\boldsymbol{b}}, \tag{42}$$

where $\mathcal{N} = \sigma_3\mathcal{M}_{12}^*(k_\star)$ and $\tilde{\boldsymbol{b}} = \sigma_2(b_3, b_4)^\mathsf{T}$. Thus the CPA solution incident from $+\infty$ (up to the normalization amplitude) can be computed directly using the antidiagonal blocks of the transfer matrix at the SS. The result (42) also means that at least one of the eigenvalues of $\mathcal{N}$ is either $+1$ or -1 and hence $\mathcal{M}_{12}(k_\star)$ has at least one nonzero eigenvalue. If additionally $\det\mathcal{M}_{12}(k_\star) = 0$, i.e., one of the eigenvalues of the block $\mathcal{M}_{12}(k_\star)$ is zero, then $\det\mathcal{N} = 0$ and we conclude that $|\mathrm{Tr}\,\mathcal{N}| = |\mathrm{Tr}\,\mathcal{M}_{12}(k_\star)| = 1$. Thus the second eigenvalue of $\mathcal{M}_{12}(k_\star)$ must be either 1 or -1. This also leaves us with only one of two possibilities discussed above in Sec. III B: If $\det\mathcal{M}_{12}(k_\star) = 0$, then $(b_3, b_4)^\mathsf{T}$ is an eigenvector of $\mathcal{M}_{21}(k_\star)$ corresponding to either 1 or -1 eigenvalue (which corroborates with the respective conclusion made above).

B. Spectral singularities of coupled waveguides

Below, for the sake of illustration, we consider the model of the optical coupler (13), with simplified piecewise constant potentials

$$V_{0,1}(x) = \begin{cases} v_{0,1}, & |x| < \ell/2 \\ 0, & |x| > \ell/2, \end{cases} \tag{43}$$

$$V_2(x) = \begin{cases} -v_2, & x \in (-\ell/2, 0) \\ v_2, & x \in (0, \ell/2) \\ 0, & |x| > \ell/2, \end{cases} \tag{44}$$

where the amplitudes $v_{0,1,2}$ are real. It has been shown above that any spectral singularity is self-dual in an odd-$\mathcal{PT}$-symmetric system. The existence of strong SSs requires simultaneous solution of four complex equations ensuring zero values of the entries of $\mathcal{M}_{jj}$, which seems to be hardly possible in our system where only four real-valued parameters are available: $v_{0,1,2}$ and ℓ. Therefore, we look for weak SSs. To this end, it is sufficient to satisfy only one equation $\det\mathcal{M}_{11}(k_\star) = 0$, and the equation $\det\mathcal{M}_{22}(k_\star) = 0$ will be satisfied automatically. Since $\det\mathcal{M}_{11}(k)$ is a complex-valued function of a real parameter k (recall we are interested only in real roots $k_\star$), in order to find a weak SS one needs at least one real-valued control parameter. As such a parameter we will use the strength of the non-Hermiticity, i.e., v_1 characterizing gain and loss (holding $v_{0,2}$ fixed). Once a SS is found, by changing a second parameter, say, v_2, one can construct a curve which shows the position of spectral singularity in a parametric space (v_1, v_2), with v_0 remaining fixed constant (all points of such a curve, however, correspond to different $k_\star$).

Without loss of generality, in what follows we will restrict our attention to $v_1 \geqslant 0$ and $v_2 \geqslant 0$. At the same time, the properties of the system depend significantly on the sign of the parameter v_0. The cases of positive and negative values of v_0 are considered separately.

1. Potential barrier $v_0 > 0$

The resulting dependences for a representative value $v_0 = 8$ are shown in Figs. 2(a) and 2(b). In order to get insight into the main features of the scattering problem, it is instructive to trace its behavior moving along the vertical axis in Fig. 2(a), which corresponds to the increase of the non-Hermiticity parameter v_1 departing from the Hermitian limit $v_1 = 0$. In the latter limit the fields $\psi_1 \pm \psi_2$ are decoupled and each is subject to an effective real potential $V_0(x) \pm V_2(x)$. The spectrum of the Hermitian system is obviously real. If the coupling strength v_2 is small enough [point a in Fig. 2(a)], then at $v_1 = 0$ the spectrum is purely continuous and fills the semiaxis $k^2 > 0$. For sufficiently large coupling v_2 [point e in Fig. 2(a)], the spectrum of the Hermitian system additionally contains a degenerate isolated eigenvalue with $k^2 < 0$ [Fig. 3(d); recall that in a system with odd-$\mathcal{PT}$ symmetry any real eigenvalue corresponds to at least two linearly independent eigenvectors, which is a direct consequence of the property $(\mathcal{PT})^2 = -1$].

Qualitatively different spectra in the Hermitian limit for small and large values of the coupling coefficient v_2 result in essentially different behaviors of the system subject to the increase of the non-Hermiticity strength v_1. If at $v_1 = 0$ the spectrum is purely real and continuous [point a in Fig. 2(a)], then it remains so for sufficiently small but nonzero v_1 [point b in Fig. 2(a)]. A further increase of v_1 results in the

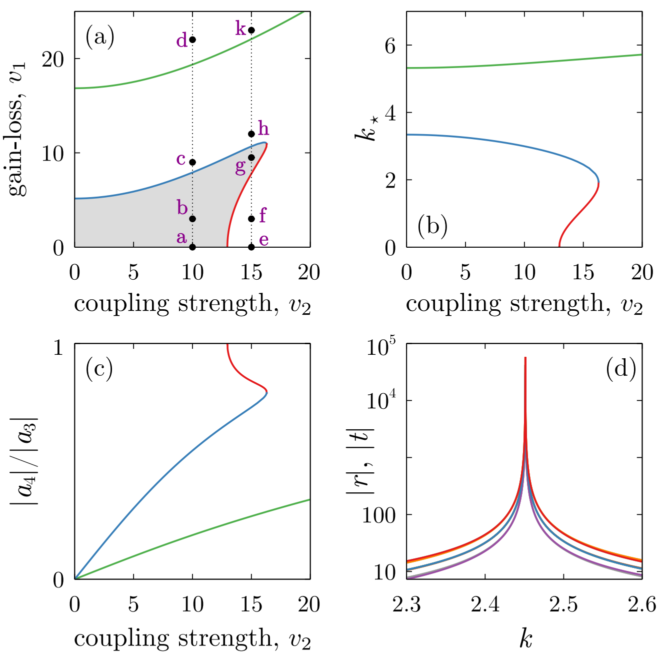

FIG. 2. Scattering by the odd-$\mathcal{PT}$-symmetric potential barrier with $v_0 = 8$ and $\ell = 1$. (a) Values of v_1 and v_2 that correspond to weak SSs are plotted as curves in the (v_1, v_2) plane. The lower (red and blue) solid lines separate the domains of unbroken (shaded area) and broken (white area) $\mathcal{PT}$-symmetric phases. The black dots labeled a–k correspond to Figs. 3(a)–3(k), respectively. (b) Weak self-dual SSs $k_\star$ as functions of the coupling strength v_2. (c) Ratio $|a_4/a_3|$ between the amplitudes of the two polarizations for the laser solution. (d) Magnitudes of reflection and transition coefficients $r^{L,R}_{\alpha\beta}$ and $t^{L,R}_{\alpha\beta}$ defined in Appendix A as functions of the wave number k driven through the self-dual SS for $v_1 \approx 10.685$ and $v_2 = 15$.

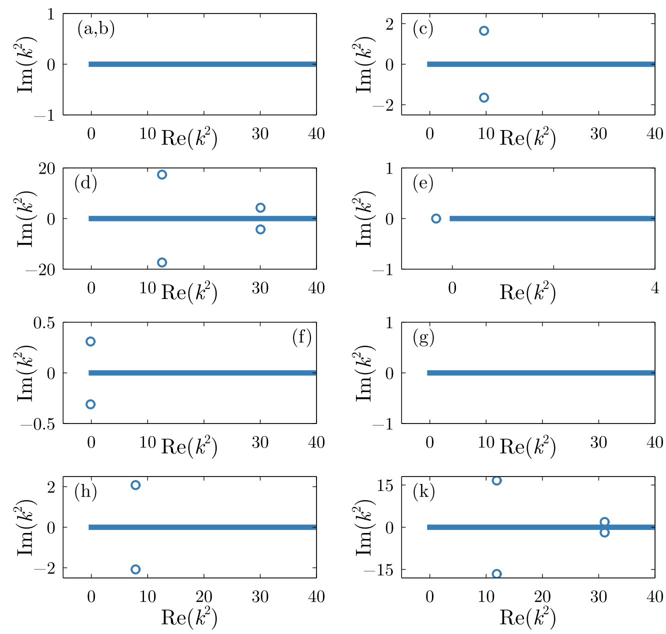

FIG. 3. Real and imaginary parts of eigenvalues for different combinations of parameters labeled with black dots in Fig. 2(a). The thick line shows the continuous spectrum and circles correspond to isolated eigenvalues.

$\mathcal{PT}$-symmetry breaking through the splitting of the self-dual SS. In Fig. 2(a) it occurs when the vertical dashed line intersects the solid curve between points b and c. As a result, a single complex-conjugate pair emerges from the continuous spectrum [see Fig. 3(b)]. This scenario of $\mathcal{PT}$-symmetry breaking through the splitting of a self-dual SS was described in [13] for a scalar scattering problem. It represents the most typical mechanism of $\mathcal{PT}$-symmetry breaking in systems without the discrete spectrum. A further increase of v_1 drives the system through a new spectral singularity which occurs when the vertical dashed line intersects the solid curve between points c and d in Fig. 2(a). In turn, for sufficiently large values of v_1, the spectrum contains two complex-conjugate pairs as shown in Fig. 3(c). It is natural to expect that a further increase of v_1 may result in new spectral singularities and new complex-conjugate pairs emerging from the continuous spectrum.

The behavior of the system becomes more complicated for larger values of the coupling strength v_2 [see points e, f, g, h, and k in Fig. 2(a) and the corresponding Figs. 3(d)–3(h), respectively]. As v_1 departs from zero, the real double isolated eigenvalue immediately splits into a complex-conjugate pair [point f in Fig. 2(a)]. This is the thresholdless $\mathcal{PT}$-symmetry breaking. However, as v_1 increases further, the complex-conjugate pair returns to the real axis; this corresponds to the SS at the intersection between the vertical dashed line and the solid $v_2(v_1)$ curve between points f and g in Fig. 2(a). Thus the increase of the non-Hermiticity parameter through the self-dual spectral singularity drives the system from a $\mathcal{PT}$ broken phase [point f in Fig. 2(a) and Fig. 3(f)] to a $\mathcal{PT}$ unbroken phase [point g in Fig. 2(a) and Fig. 3(g)]. Hence we encounter a rather interesting situation when the increase of the non-Hermiticity strength leads to the restoration of unbroken $\mathcal{PT}$ symmetry through the coalescence of two isolated complex-conjugate eigenvalues at a self-dual spectral singularity. This effect is opposite to the $\mathcal{PT}$-symmetry breaking through the splitting of a self-dual SS. A further increase of v_1 triggers a new self-dual SS [at the intersection between the dashed line and the solid curve between points g and h, as shown in Fig. 3(h)], which results in the $\mathcal{PT}$-symmetry breaking with a new complex-conjugate pair of eigenvalues emerging from the continuous spectrum. Next the increase of v_1 from point h to point k results in a new spectral singularity, where the second complex-conjugate pair emerges [see Fig. 3(k)].

To give a physical interpretation for the splitting of a self-dual SS, let us recall the relations (25) and (27). If Im $k_0 < 0$, where k_0 is a zero of det $\mathcal{M}_{11}(k_0) = 0$ and det $\mathcal{M}_{22}(k_0^*) = 0$, the system allows for a solution $\boldsymbol{\psi}_-$ that transforms into the CPA solution at Im$k_0 \to -0$ and outside the potential, i.e., at $|x| > \ell/2$, can be written as

$$\boldsymbol{\psi}_- = e^{ik_0x}[M_{12}(k_0)|\uparrow\rangle - M_{11}(k_0)|\downarrow\rangle], \quad x < -\frac{\ell}{2},$$

$$\boldsymbol{\psi}_- = e^{-ik_0x}[M_{12}(k_0)|\uparrow\rangle + M_{11}(k_0)|\downarrow\rangle], \quad x > \frac{\ell}{2}. \qquad (45)$$

as well as for a solution $\boldsymbol{\psi}_+$ which transforms into the lasing solution in the limit $\mathrm{Im}k_0 \to -0$:

$$\boldsymbol{\psi}_+ = e^{-ik_0^* x}[M_{34}(k_0)|\uparrow\rangle - M_{33}(k_0)|\downarrow\rangle], \quad x < -\frac{\ell}{2},$$
$$\boldsymbol{\psi}_+ = e^{ik_0^* x}[M_{34}(k_0)|\uparrow\rangle + M_{33}(k_0)|\downarrow\rangle], \quad x > \frac{\ell}{2}. \quad (46)$$

These are spatially localized solutions with the complex energies $E = k_0^2$ [Eq. (45)] and $E = [k_0^*]^2$ [Eq. (46)]. In optical applications, where $-E = \beta$ (see the discussion in Sec. II) is the propagation constant, these solutions represent propagating beams whose intensity decays in the case (45) and grows in the case (46), along propagation (i.e., along the z axis). Therefore, they are loosely referred to as bound states in a continuum (BIC) [13,27] (which should not be confused with BIC in the conventional mathematical sense, which are spatially localized eigenstates with real energy embedded in the continuous spectrum [28]). Such localized growing solutions can also be viewed as the development of the convective instability, which is well known in kinetic theory [29].

Coherent perfect absorption and lasing solutions are superpositions of two polarizations. The amplitudes of different polarizations are related to each other by the formula

$$-\frac{a_1}{a_2} = \frac{b_3}{b_4} = \frac{M_{12}(k_\star)}{M_{11}(k_\star)} \quad (47)$$

for the CPA solution and by the formula

$$-\frac{a_3}{a_4} = \frac{b_1}{b_2} = \frac{M_{11}^*(k_\star)}{M_{12}^*(k_\star)} \quad (48)$$

for the lasing solution. Numerically we obtained that the amplitude ratio between up and down polarization is always below unity $|a_4/a_3| = |b_2/b_1| < 1$ [shown in Fig. 2(c)]. Physically, this is an expected result; it means that the laser solution is dominantly concentrated in the mode $|\uparrow\rangle$, i.e., in the waveguide with gain. Conversely, for the CPA solution the spin-down component dominates, which means that the respective solutions are concentrated in the lossy waveguide. Interestingly, the relations between the amplitudes of polarizations have different slopes for SS belonging to different branches of the SS. Comparing Fig. 2(c) with Figs. 2(a) and 2(b), we observe that the SS emerging from the coalescing isolated complex eigenvalues (the red lines) has a larger relation $|a_4/a_3|$ as compared with the SS emerging from the continuous spectrum (blue and green lines).

Finally, computing the left and right reflection and transmission coefficients (see Appendix A), we observe that all of them diverge simultaneously as the system is driven through the self-dual SS, as illustrated in Fig. 2(d), where we plot the amplitudes of all 16 coefficients $r_{\alpha\beta}^{L,R}$ and $t_{\alpha\beta}^{L,R}$ as functions of k with all other parameters kept fixed and corresponding to a spectral singularity at $k_\star \approx 2.451$. Notice that some of the scattering coefficients have equal amplitudes; hence the number of curves visible in Fig. 2(d) is less than 16.

2. Potential well $v_0 < 0$

The behavior of the system is significantly different for the scattering by a potential well, which corresponds to negative values of v_0. Choosing as a representative example $v_0 = -3$, we illustrate the spectral singularities and the corresponding eigenvalue diagrams in Figs. 4 and 5. Starting from the Hermitian limit $v_1 = 0$, we observe that for any value of the coupling strength v_2 the Hermitian system contains an isolated double eigenvalue [see point a in Fig. 4(a) and the corresponding spectrum shown in Fig. 5(a)]. The nonzero non-Hermiticity parameter v_1, even infinitesimal, immediately results in the splitting of the double eigenvalue in a complex-conjugate pair [see point b in Fig. 4(a) and the spectrum in Fig. 5(b)]. Thus the $\mathcal{PT}$-symmetry breaking in this case is thresholdless. A further increase of v_1 drives the system through a self-dual SS, which results in the emergence of a new complex-conjugate pair [point c in Fig. 4(a) and Fig. 5(c)]. Thus, in the scattering by the potential well, the splitting of the self-dual SS into a complex-conjugate pair occurs, but it does not represent the boundary between the unbroken and broken $\mathcal{PT}$ symmetry, the latter being broken already for any nonzero non-Hermiticity strength v_1.

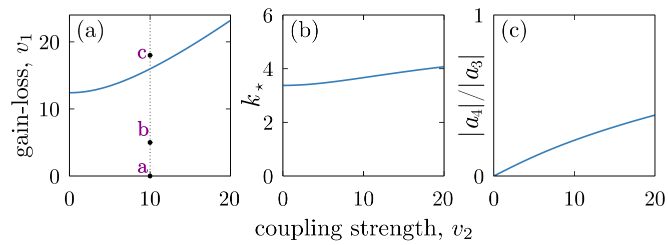

FIG. 4. Scattering on the odd-$\mathcal{PT}$-symmetric potential well with $v_0 = -3$ and $\ell = 1$. (a) Values of v_1 and v_2 that correspond to weak SSs are plotted as curves in the (v_1, v_2) plane. (b) Dependence of $k_\star$ on the coupling strength v_2. (c) Ratio $|a_4/a_3|$ between amplitudes of the two polarizations of the lasing solution. Black dots labeled a–c correspond to Figs. 5(a)–5(c), respectively. Here $\mathcal{PT}$ symmetry is broken for any $v_1 > 0$ with one or more complex-conjugate pairs in the spectrum.

Additionally, we note that the dependence $v_1(v_2)$ corresponding to the spectral singularities increases monotonically [Fig. 5(a)], the wave number $k_\star$ depends weakly on the coupling strength v_2 [Fig. 5(b)], and the ratio between the amplitudes of two polarizations of the lasing solution [and of the CPA solution, as it follows from (47) and (48)] increases with v_2 too [Fig. 5(c)].

C. Comparison with the even-$\mathcal{PT}$-symmetric coupling

To highlight the peculiarities of the scattering by odd-$\mathcal{PT}$-symmetric potentials, we complement the results collected above with the analysis of a similar system, but coupled by

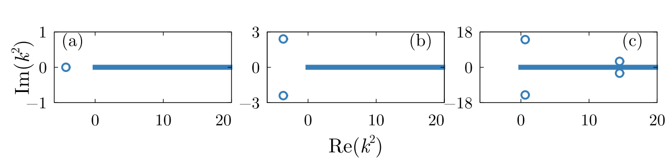

FIG. 5. Real and imaginary parts of eigenvalues for different combinations of parameters labeled with black dots in Fig. 4(a). The thick line shows the continuous spectrum and circles correspond to isolated eigenvalues.

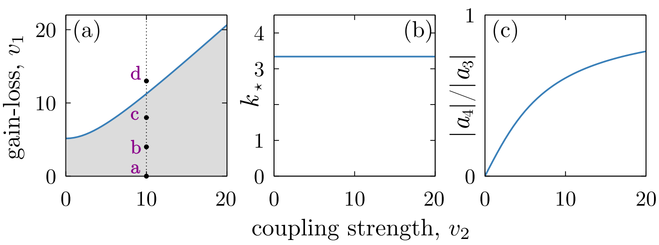

FIG. 6. Scattering by the even-$\mathcal{PT}$-symmetric potential barrier with $v_0 = 8$ and $\ell = 1$. (a) Values of v_1 and v_2 that correspond to weak SSs are plotted as curves in the (v_1, v_2) plane and separate the unbroken $\mathcal{PT}$-symmetric phase (shaded domain) and the broken one (white domain). The black dots labeled a–d correspond to Figs. 7(a)–7(d), respectively. (b) Weak SS vs coupling strength. (c) Ratio $|a_4/a_3|$ between amplitudes of the two polarizations of the laser solution.

a homogeneous (symmetric) medium. More specifically, we consider the model (13)–(36), but with the even function $V_2(x)$ in the form [cf. (44)]

$$V_2(x) = \begin{cases} v_2, & x \in (-\ell/2, \ell/2) \\ 0, & |x| > \ell/2. \end{cases} \tag{49}$$

Notice that this modification of the model affects only the total symmetry, but does not affect distribution of gain and losses. The resulting system is invariant under the conventional (even-)parity-time reversal with the parity operator being $\mathcal{P} = \sigma_1$ and the bosonic time reversal $\mathcal{T} = \mathcal{K}$. At the same time, the new system does not respect the odd-$\mathcal{PT}$ symmetry introduced above.

1. Potential barrier $v_0 > 0$

The results are summarized in Figs. 6 and 7. Starting from the Hermitian limit, we observe that the spectrum is purely real and continuous for small values of the coupling v_2. However, for larger values of v_2, the spectrum does contain one or more isolated eigenvalues. In contrast to the odd-$\mathcal{PT}$ case, the isolated eigenvalues are generically simple. For the sake of illustration, we choose coupling strength $v_2 = 10$, which corresponds to a single isolated eigenvalue in the Hermitian limit [point a in Fig. 6(a) and Fig. 7(a)]. As v_1 departs from zero, the isolated eigenvalue remains real and moves towards the edge of the continuous spectrum [point b in Fig. 6(a) and Fig. 7(b)] and eventually merges with the continuous spectrum. At this instant the spectrum becomes purely real and continuous [point c in Fig. 6(a) and Fig. 7(c)]. A further increase v_1 from point c to point d leads to a self-dual spectral singularity which results in the $\mathcal{PT}$-symmetry breaking with a pair of complex-conjugate eigenvalues emerging from the continuous spectrum [point d in Fig. 6(a) and Fig. 7(d)].

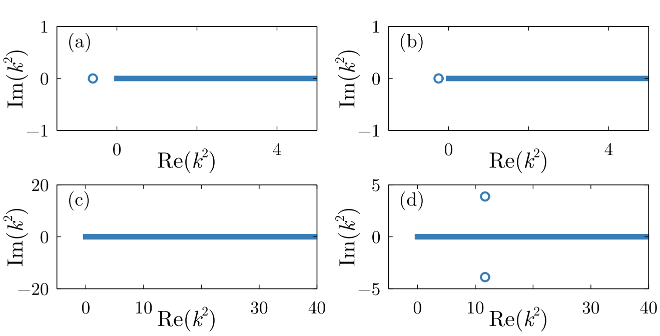

FIG. 7. Real and imaginary parts of eigenvalues for different combinations of parameters labeled with black dots in Fig. 6(a). The thick line shows the continuous spectrum and circles correspond to isolated eigenvalues.

The described behavior of the discrete eigenvalues and SSs for the even-$\mathcal{PT}$-symmetric coupler features several distinctive differences from those for the odd-$\mathcal{PT}$-symmetric coupler, described above. First, in the case of even-$\mathcal{PT}$ symmetry we observe that dependence $v_1(v_2)$ (which separates unbroken and broken phases) is monotonic [see Fig. 6(a)]. This is expectable, because the system is locally (i.e., at each given x) $\mathcal{PT}$ symmetric and thus the $\mathcal{PT}$ phase transition for larger values of coupling v_2 is expected at larger gain and losses v_1. In the case of odd-$\mathcal{PT}$ symmetry [Fig. 2(a)] two new, somehow opposite, effects appear. At any value of gain and loss, i.e., of v_1, the increase of the coupling v_2 results in $\mathcal{PT}$-symmetry breaking. Moreover, in some intervals of the coupling constant values, there exist two different values of the gain-and-loss coefficient v_1 for which spectral singularities can be found. Thus, for the coupling v_2 in this interval, the increase of the non-Hermiticity parameter v_1 can stabilize the odd-$\mathcal{PT}$-symmetric system, in sharp contrast to the destabilizing effect of growing v_1 (at fixed v_2) in the case of even-$\mathcal{PT}$ symmetry. In the case of the odd-$\mathcal{PT}$ symmetry for a given v_1 lying in certain specific intervals it is possible to obtain two spectral singularities, unlike what happens in the case of even-$\mathcal{PT}$ symmetry. Also we observe that for the even coupling $k_\star$ does not depend on v_2 and the ratio between $|a_4|$ and $|a_3|$ computed for the laser solution grows monotonically and slowly approaches unity.

When there is more than one eigenvalue in the Hermitian limit ($v_1 = 0$), an increase of v_1 leads to its successive immersion in the continuous spectrum such that after the last discrete eigenvalue is merged with the continuum, the spectrum remains purely continuous and real until the SS is formed. That is why the splitting of the self-dual SS always represents the boundary between unbroken and broken $\mathcal{PT}$ symmetry [i.e., between shaded and white areas in Fig. 6(a)].

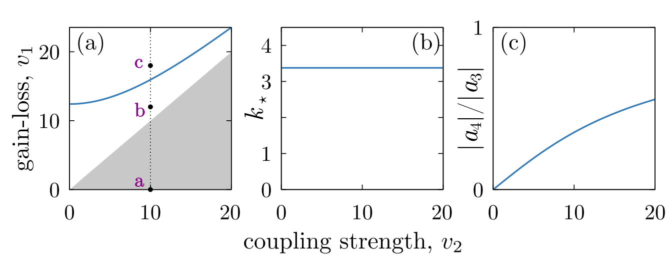

FIG. 8. Scattering by the even-$\mathcal{PT}$-symmetric potential well with $v_0 = -3$ and $\ell = 1$. (a) Values of v_1 and v_2 that correspond to weak SSs are plotted as curves in the (v_1, v_2) plane. Shaded and white domains correspond to the unbroken and broken $\mathcal{PT}$-symmetric phase, respectively. The black dots labeled a–c correspond to Figs. 9(a)–9(c), respectively. (b) Weak SS vs the coupling strength v_2. (c) Ratio $|a_4/a_3|$ between amplitudes of the two polarizations of the laser solution.

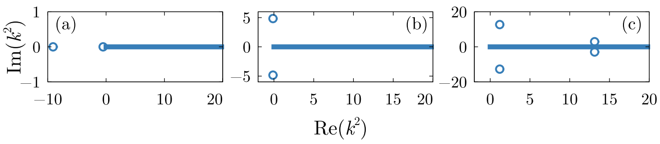

FIG. 9. Real and imaginary parts of eigenvalues for different combinations of parameters labeled with black dots in Fig. 8(a). The thick line shows the continuous spectrum and circles correspond to isolated eigenvalues.

2. Potential well $v_0 < 0$

In the Hermitian limit $v_1 = 0$, the spectrum of the potential $\hat{U}(x)$ with nonzero coupling $v_2 > 0$ contains the discrete part consisting of two or more eigenvalues (depending on the depth of the well $|v_0|$ and on the coupling strength v_2) which are generically simple. The increase of v_1 leads to the $\mathcal{PT}$-symmetry breaking through the exceptional point scenario: At the threshold value of v_1, all real eigenvalues collide pairwise and simultaneously and then split into one (or several, if the well is deep enough) complex-conjugate pair. The representative diagrams with $v_0 = -3$ (which corresponds to two real isolated eigenvalues in the Hermitian limit) are presented in Figs. 8 and 9. The phase transition corresponds to the boundary between shaded and white domains in Fig. 8(a). It is also illustrated by the transition between points a and b in Fig. 8(a), as well as by transition between Figs. 9(a) and 9(b). The value of non-Hermiticity v_1 where the exceptional point transition takes place is always below the value of v_1 corresponding to the self-dual SS, the latter shown by the blue solid line in Fig. 8(a).

VI. DISCUSSION AND CONCLUSION

In this work we have developed formalism for the scattering of the two-component field by localized (matrix) potentials obeying odd-$\mathcal{PT}$ symmetry. Being two-component fields, the reflected and transmitted fields have spinor character and can be characterized by two opposite polarizations. The resulting problem is described by a 4×4 transfer matrix, which is naturally represented in the form of a 2×2 block matrix, where the blocks describe reflection, transmission, and transformation of waves with either of two polarizations. The odd-$\mathcal{PT}$-symmetry relates two diagonal, as well as two antidiagonal, blocks.

We identified two types of spectral singularities in such a system. If the determinants of diagonal blocks vanish, one deals with a weak singularity, for which lasing or CPA solutions are characterized by interrelated amplitudes of the polarizations incident or absorbed from one side of the potential. If the diagonal blocks are zero matrices, one deals with a strong singularity, for which no constraints on the relations between the amplitudes are imposed. In any of these cases, spectral singularities are self-dual.

As an example we considered a simple odd-$\mathcal{PT}$-symmetric dispersive coupler with antisymmetric coupling. The available parameters were not enough to obtain strong spectral singularity, but allowed for a detailed study of weak self-dual spectral singularities, as well as for the demonstration of the odd-$\mathcal{PT}$-symmetry breaking through the splitting of self-dual spectral singularities. We also found that in some cases the increase of the non-Hermiticity strength can lead to the restoration of the unbroken $\mathcal{PT}$ symmetry, which corresponds to the situation when two complex-conjugate eigenvalues coalesce at the real axis and form a self-dual spectral singularity. Apart from the phase transition through the spectral singularity, our simple odd-$\mathcal{PT}$-symmetric system features two other mechanisms of the transition from a purely real to a complex spectrum. One of these mechanisms is the well-studied coalescence of two isolated eigenvalues at the exceptional point, where the Hamiltonian becomes nondiagonalizable, with the ensuing splitting of the multiple eigenvalue into a complex-conjugate pair. Another encountered scenario corresponds to the splitting of a degenerate semisimple eigenvalue (with algebraic and geometric multiplicities equal to 2) into a complex-conjugate pair (this situation is distinctively different from the exceptional point scenario because the Hamiltonian with the semisimple eigenvalue remains diagonalizable).

We have also compared properties of the odd-$\mathcal{PT}$-symmetric coupler with its even-$\mathcal{PT}$-symmetric counterpart, which revealed significant qualitative differences in the scattering properties of the two systems. We can also point out some rather general features that hold for either even- and odd-$\mathcal{PT}$-symmetric systems. In particular, we observe that in the parametric vicinity of each self-dual spectral singularity, the spectrum either is purely continuous or contains one or several complex-conjugate pairs (a similar observation for the one-component scattering problem with the conventional even-$\mathcal{PT}$ symmetry was recently pointed out in [30]). Another intriguing observation is that for all considered cases complex-conjugate pairs of eigenvalues never coexist with real isolated eigenvalues. Additionally, while for the scattering by the potential barrier the splitting of self-dual singularity can represent the boundary between unbroken and broken $\mathcal{PT}$ symmetry, i.e., the phase transition occurs through the splitting of the spectral singularity, for the scattering by the potential well the $\mathcal{PT}$-symmetry breaking never occurs through the splitting of the self-dual spectral singularity. Instead, it is caused by a different mechanism (i.e., by the splitting of multiple isolated eigenvalues into complex-conjugate pairs). As a result, for a system with the potential well, the splitting of a spectral singularity results in the emergence of a new complex-conjugate pair of complex eigenvalues in the already broken $\mathcal{PT}$-symmetric phase.

ACKNOWLEDGMENT

The research of D.A.Z. was supported by the government of the Russian Federation (Grant No. 08-08).

APPENDIX A: SCATTERING DATA THROUGH THE TRANSFER-MATRIX ELEMENTS

Introducing

$$\Delta = M_{33}M_{44} - M_{34}M_{43},$$

we have the left incidence

$$r^L_{\uparrow\uparrow} = \frac{M_{34}M_{41} - M_{31}M_{44}}{\Delta}, \quad r^L_{\uparrow\downarrow} = \frac{M_{31}M_{43} - M_{33}M_{41}}{\Delta},$$
$$r^L_{\downarrow\uparrow} = \frac{M_{42}M_{34} - M_{32}M_{44}}{\Delta}, \quad r^L_{\downarrow\downarrow} = \frac{M_{32}M_{43} - M_{42}M_{33}}{\Delta},$$
$$t^L_{\uparrow\uparrow} = M_{11} + M_{13}r^L_{\uparrow\uparrow} + M_{14}r^L_{\uparrow\downarrow}, \quad t^L_{\uparrow\downarrow} = M_{21} + M_{23}r^L_{\uparrow\uparrow} + M_{24}r^L_{\uparrow\downarrow},$$
$$t^L_{\downarrow\uparrow} = M_{12} + M_{13}r^L_{\downarrow\uparrow} + M_{14}r^L_{\downarrow\downarrow}, \quad t^L_{\downarrow\downarrow} = M_{22} + M_{23}r^L_{\downarrow\uparrow} + M_{24}r^L_{\downarrow\downarrow}$$

and right incidence

$$r^R_{\uparrow\uparrow} = \frac{M_{13}M_{44} - M_{14}M_{43}}{\Delta}, \quad r^R_{\uparrow\downarrow} = \frac{M_{23}M_{44} - M_{24}M_{43}}{\Delta},$$
$$r^R_{\downarrow\uparrow} = \frac{M_{33}M_{14} - M_{13}M_{34}}{\Delta}, \quad r^R_{\downarrow\downarrow} = \frac{M_{24}M_{33} - M_{23}M_{34}}{\Delta},$$
$$t^R_{\uparrow\uparrow} = \frac{M_{44}}{\Delta}, \quad t^R_{\uparrow\downarrow} = -\frac{M_{43}}{\Delta}, \quad t^R_{\downarrow\uparrow} = -\frac{M_{34}}{\Delta}, \quad t^R_{\downarrow\downarrow} = \frac{M_{33}}{\Delta}.$$

APPENDIX B: INVERSE OF THE BLOCK MATRIX

For the sake of convenience, here we present the explicit formulas for the inverse of a block matrix [25,31]. Consider

$$M = \begin{pmatrix} \mathcal{M}_{11} & \mathcal{M}_{12} \\ \mathcal{M}_{21} & \mathcal{M}_{22} \end{pmatrix}, \tag{B1}$$

where $\mathcal{M}_{ij}$ are 2×2 matrices. Assume that $\mathcal{M}_{11}$ is nonsingular. Then M is invertible if and only if matrix $\mathcal{C}_1$, defined as $\mathcal{C}_1 = \mathcal{M}_{22} - \mathcal{M}_{21}\mathcal{M}_{11}^{-1}\mathcal{M}_{12}$, is invertible and

$$M^{-1} = \begin{pmatrix} \mathcal{M}_{11}^{-1} + \mathcal{M}_{11}^{-1}\mathcal{M}_{12}\mathcal{C}_1^{-1}\mathcal{M}_{21}\mathcal{M}_{11}^{-1} & -\mathcal{M}_{11}^{-1}\mathcal{M}_{12}\mathcal{C}_1^{-1} \\ -\mathcal{C}_1^{-1}\mathcal{M}_{21}\mathcal{M}_{11}^{-1} & \mathcal{C}_1^{-1} \end{pmatrix}. \tag{B2}$$

Assume that $\mathcal{M}_{22}$ is nonsingular. Then M is invertible if and only if matrix $\mathcal{C}_2$, defined as $\mathcal{C}_2 = \mathcal{M}_{11} - \mathcal{M}_{12}\mathcal{M}_{22}^{-1}\mathcal{M}_{21}$, is invertible and

$$M^{-1} = \begin{pmatrix} \mathcal{C}_2^{-1} & -\mathcal{C}_2^{-1}\mathcal{M}_{12}\mathcal{M}_{22}^{-1} \\ -\mathcal{M}_{22}^{-1}\mathcal{M}_{21}\mathcal{C}_2^{-1} & \mathcal{M}_{22}^{-1} + \mathcal{M}_{22}^{-1}\mathcal{M}_{21}\mathcal{C}_2^{-1}\mathcal{M}_{12}\mathcal{M}_{22}^{-1} \end{pmatrix}. \tag{B3}$$

[1] A. P. Khapalyuk, Dokl. Akad. Nauk SSSR **6**, 301 (1962); Opt. Spectrosk. **52**, 194 (1982).

[2] N. N. Rosanov, Antilaser: Resonance absorption mode or coherent perfect absorption? Phys. Usp. **60**, 818 (2017).

[3] L. Poladian, Resonance mode expansions and exact solutions for nonuniform gratings, Phys. Rev. E **54**, 2963 (1996).

[4] Y. D. Chong, L. Ge, H. Cao, and A. D. Stone, Coherent Perfect Absorbers: Time-Reversed Lasers, Phys. Rev. Lett. **105**, 053901 (2010); W. Wan, Y. Chong, L. Ge, H. Noh, A. D. Stone, and H. Cao, Time-reversed lasing and interferometric control of absorption, Science **331**, 889 (2011).

[5] D. G. Baranov, A. Krasnok, T. Shegai, A. Alú, and Y. D. Chong, Coherent perfect absorbers: Linear control of light with light, Nat. Rev. Mater. **2**, 17064 (2017).

[6] A. Mostafazadeh, Spectral Singularities of Complex Scattering Potentials and Infinite Reflection and Transmission Coefficients at Real Energies, Phys. Rev. Lett. **102**, 220402 (2009).

[7] Z. Ahmed, Zero width resonance (spectral singularity) in a complex PT-symmetric potential, J. Phys. A: Math. Theor. **42**, 472005 (2009).

[8] M. A. Naimark, Investigation of the spectrum and the expansion in eigenfunctions of a nonselfadjoint operator of the second order on a semi-axis, Tr. Mosk. Mat. Obs. **3**, 181 (1954); J. Schwartz, Some non-selfadjoint operators, Commun. Pure Appl. Math. **13**, 609 (1960); B. Vainberg, On the analytical properties of the resolvent for a certain class of operator-pencils, Math. USSR Sb. **6**, 241 (1968); G. S. Guseinov, On the concept of spectral singularities, Pramana J. Phys. **73**, 587 (2009).

[9] S. Longhi, $\mathcal{PT}$-symmetric laser absorber, Phys. Rev. A **82**, 031801 (2010).

[10] A. Mostafazadeh, Self-dual spectral singularities and coherent perfect absorbing lasers without $\mathcal{PT}$-symmetry, J. Phys. A: Math. Theor. **45**, 444024 (2012).

[11] C. M. Bender and S. Boettcher, Real Spectra in Non-Hermitian Hamiltonians Having $\mathcal{PT}$-Symmetry, Phys. Rev. Lett. **80**, 5243 (1998); C. M. Bender, Making sense of non-Hermitian Hamiltonians, Rep. Prog. Phys. **70**, 947 (2007).

[12] Y. D. Chong, L. Ge, and A. D. Stone, $\mathcal{PT}$-Symmetry Breaking and Laser-Absorber Modes in Optical Scattering Systems, Phys. Rev. Lett. **106**, 093902 (2011).

[13] V. V. Konotop and D. A. Zezyulin, Phase transition through the splitting of self-dual spectral singularity in optical potentials, Opt. Lett. **42**, 5206 (2017).

[14] A. Mostafazadeh and H. Mehri-Dehnavi, Spectral singularities, biorthonormal systems and a two-parameter family of complex point interactions, J. Phys. A: Math. Theor. **42**, 125303 (2009).

[15] T. Kato, *Perturbation Theory for Linear Operators* (Springer, Berlin, 1966)

[16] C. M. Bender, M. V. Berry, and A. Mandilara, Generalized PT symmetry and real spectra, J. Phys. A: Math. Gen. **35**, L467 (2002); W. D. Heiss, The physics of exceptional points, J. Phys. A: Math. Theor. **45**, 444016 (2012).

[17] J. Yang, Classes of non-parity-time-symmetric optical potentials with exceptional-point-free phase transitions, Opt. Lett. **42**, 4067 (2017).

[18] A. Messiah, *Quantum Mechanics* (Wiley, New York, 1966), Vol. II.

[19] V. V. Konotop, J. Yang, and D. A. Zezyulin, Nonlinear waves in $\mathcal{PT}$-symmetric systems, Rev. Mod. Phys. **88**, 035002 (2016).

[20] K. Jones-Smith and H. Mathur, Non-Hermitian quantum Hamiltonians with $\mathcal{PT}$ symmetry, Phys. Rev. A **82**, 042101 (2010).

[21] C. M. Bender and S. P. Klevansky, $\mathcal{PT}$-symmetric representations of fermionic algebras, Phys. Rev. A **84**, 024102 (2011).

[22] V. V. Konotop and D. A. Zezyulin, Odd-Time Reversal $\mathcal{PT}$ Symmetry Induced by Anti-$\mathcal{PT}$-Symmetric Medium, Phys. Rev. Lett. **120**, 123902 (2018).

[23] L. Ge and H. E. Tureci, Antisymmetric $\mathcal{PT}$-photonic structures with balanced positive-negative-index materials, Phys. Rev. A **88**, 053810 (2013).

[24] V. V. Konotop, in *Parity-Time Symmetry and Its Applications*, edited by D. Christodoulides and J. Yang, Springer Tracts in Modern Physics (Springer Nature, Singapore, 2018), Vol. 280, pp. 407–441.

[25] T.-T. Lu and S.-H. Shiou, Inverses of 2×2 block matrices, Comput. Math. Appl. **43**, 119 (2002).

[26] C. Hang, G. Huang, and V. V. Konotop, Tunable spectral singularities: Coherent perfect absorber and laser in an atomic medium, New J. Phys. **18**, 085003 (2016).

[27] S. Longhi, Bound states in the continuum in $\mathcal{PT}$-symmetric optical lattices, Opt. Lett. **39**, 1697 (2014); S. Garmon, M. Gianfreda, and N. Hatano, Bound states, scattering states, and resonant states in $\mathcal{PT}$-symmetric open quantum systems, Phys. Rev. A **92**, 022125 (2015); Y. V. Kartashov, C. Milián, V. V. Konotop, and L. Torner, Bound states in the continuum in a two-dimensional $\mathcal{PT}$-symmetric system, Opt. Lett. **43**, 575 (2018).

[28] J. von Neumann and E. Wigner, Über merkwürdige diskrete eigenwerte, Phys. Z. **30**, 465 (1929); F. H. Stillinger and D. R. Herrick, Bound states in the continuum, Phys. Rev. A **11**, 446 (1975); H. Friedrich and D. Wintgen, Interfering resonances and bound states in the continuum, *ibid.* **32**, 3231 (1985); J. Pappademos, U. Sukhatme, and A. Pagnamenta, Bound states in the continuum from supersymmetric quantum mechanics, *ibid.* **48**, 3525 (1993); T. A. Weber and D. L. Pursey, Continuum bound states, *ibid.* **50**, 4478 (1994).

[29] E. M. Lifshitz and L. P. Pitaevskii, *Physical Kinetics* (Pergamon Press, Oxford, 1981).

[30] Z. Ahmed, S. Kumar, and D. Gosh, Three types of discrete energy eigenvalues in complex PT-symmetric scattering potentials, Phys. Rev. A **98**, 042101 (2018).

[31] B. Noble and J. W. Daniel, *Applied Linear Algebra*, 3rd ed. (Prentice-Hall, Englewood Cliffs, 1988).